*32nd EPS Conference on Plasma Phys. Tarragona, 27 June - 1 July 2005 ECA Vol.**29C**, P-1.054 (2005)*

Numerical Plasma Edge MHD Stability Analysis Revisited

O. Kwon and S. Saarelma* and JET-EFDA contributors[†]
Dept. Of Physics, Daegu University, Gyungbuk, Korea
*EURATOM/UKAEA Fusion Association, Culham Science Centre,
Abingdon, Oxon. UK OX14 3DB

Abstract

We have recalculated the MHD stability of a JET discharge in the diagnostic optimised configuration. Previous results using the MISHKA-I stability code have shown that the reconstructed equilibrium of the experiment lies in the stable region against low to intermediate *n* peeling-ballooning modes after the ELM crash, and in the unstable region just before the crash. More detailed stability analysis using the ELITE code has been carried out in this study, and good agreement with previous results has been found. The stable region in *s*-α space gets narrower for higher *n* values.

Introduction

During the high confinement regime or the H-mode, a regular sequence of periods of MHD activity including rapid loss of particles and energy from the edge region occurs. These activities, known as edge localized modes (ELMs), can deteriorate the global confinement but are efficient in removing density and impurities. It is therefore desirable to understand the physics of the underlying ELM activity.

One of the main results found in a previous study [1] using the MISHKA-I stability code [2] for the JET diagnostic optimized configuration discharges [3] was that just before an ELM, the equilibrium lies in the region unstable to low- to intermediate-*n* peeling ballooning modes, and second stable to high-*n* ballooning modes due to low shear. After an ELM crash, the flattening of the pressure gradient makes the plasma return to the low- to intermediate-*n* stable region.

We have revisited the plasma edge stability analysis of a discharge, using the 2-D linearized ideal MHD stability code, ELITE [4]. The computing time can be significantly reduced with this code, and ELITE allows the analysis to be extended to higher toroidal mode number, *n*, without computations requiring excessive CPU time.

[†]see appendix of J.Pamela et al., Fusion Energy 2004 (Proc. 20th Int. Conf. Vilamoura, 2004) IAEA, Vienna (2004).

Equilibrium Reconstruction and Stability Analysis

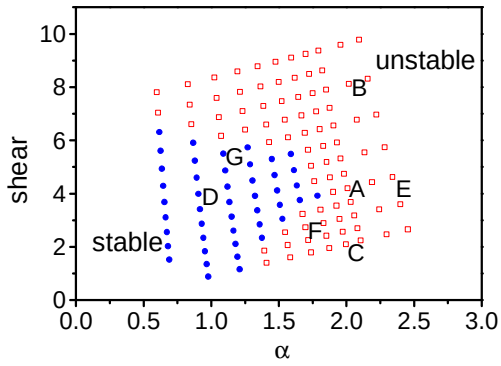

Figure 1. MHD stability of a JET diagnostic optimized configuration shot 55937 just before the type I ELM crash for n=6. Open squares are unstable points and solid circles are stable ones. The point A corresponds to a reconstruction of experimental equilibrium.

The equilibrium reconstruction needed for the stability calculation is described in detail in Ref. [1]. To briefly summarize, the edge LIDAR Thomson scattering and ECE radiometer, with edge CXRS (charge exchange recombination) as extra information, have been used for the edge electron temperature profiles. The edge LIDAR and lithium beam diagnostics have been used to determine the edge density profiles. The core electron temperature and density profiles have been obtained with the LIDAR Thomson scattering. For ion pressure profiles, $P_{electron}=P_{ion}$ has been assumed. The inductively driven current and the pressure gradient driven bootstrap current has been calculated self-consistently with the HELENA equilibrium code. The bootstrap current dominates the inductive current in the edge region where the stability of ballooning-peeling mode determines the ELM properties.

The peeling-ballooning stability has been determined with the 2-D linearized ideal MHD stability code, ELITE, which employs an extension of classical ballooning expansion and which uses a second order expansion in *1/n*. We have chosen 2ms before the ELM crash of the JET shot 55937. The MHD stability boundary calculated with the ELITE code for $n=6$ is shown in Fig. 1 in the usual s-α space, where $s=(dq/dr)/(r/q)$ is the magnetic shear and $\alpha=-2\mu_0 Rq^2(dp/dr)/B^2$ is the normalised pressure gradient. Both quantities are evaluated for $\psi=0.98$ at the outboard side on the mid-plane (ψ is normalised poloidal flux). In Fig. 1, the solid circles represent the stable equilibria and the open squares the unstable ones. The results are in good agreement, both qualitatively and quantitatively, with previous calculations [1], where the MISHKA-1 code had been used for stability determination. The unstable point denoted by A in Fig. 1 corresponds to the experimental equilibrium. This point A is deep in the unstable region for the peeling-ballooning stability. However it lies in the second stable region for infinite-n ballooning modes. The mode structure shows rather extended peeling-ballooning characteristics as in Ref. [1]. This is consistent with the experiment, in that type I ELM activity with large energy loss has been observed in this shot. Other equilibria to be used in the stability scan are generated by changing the weight on $dp/d\psi$ and the current with

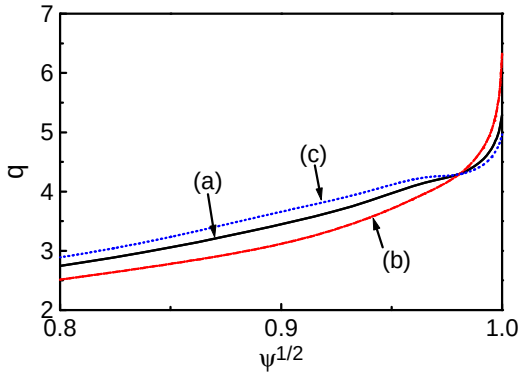

Figure 2. q-profiles as a function of $\psi^{1/2}$ for
(a) equilibrium point A of Fig. 1,
(b) equilibrium point B of Fig. 1, and
(c) equilibrium point C of Fig. 1

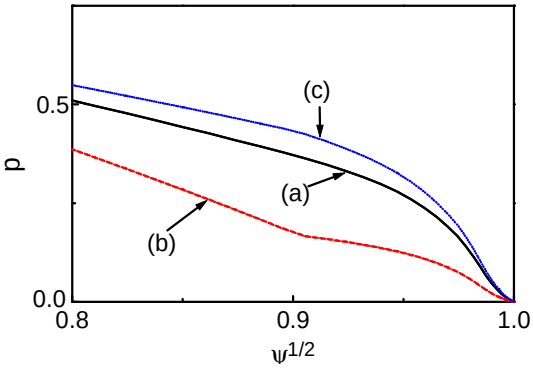

Figure 3. Pressure profiles in arbitrary units as a function of $\psi^{1/2}$ for:
(a) equilibrium point A of Fig. 1,
(b) equilibrium point D of Fig. 1, and
(c) equilibrium point E of Fig. 1

a step function in the region $\psi>0.95$. After the ELM crash, the equilibrium is located in the stable region of Fig. 1.

The *q*-profiles for different current profiles with similar pressure gradient profiles are shown in Fig. 2 as a function of $\psi^{1/2}$. The *q*-profiles of (a), (b) and (c) in Fig. 2 correspond to the equilibrium points of A, B and C (i.e., points with similar α) in Fig. 1, respectively. Although the global *q* profiles do not change much, they change considerably, and therefore so does *s*, near the $\psi=0.98$ surface. The pressure profiles for different pressure gradient profiles with similar current profiles are shown in Fig. 3 as a function of $\psi^{1/2}$. The pressure profiles of (a), (b) and (c) in Fig. 3 correspond to the equilibrium points of A, D and E (i.e., points with similar *s*) in Fig. 1, respectively. The α values near the $\psi=0.98$ surface differ considerably for these points.

Results for higher-*n* calculations are shown in Fig. 4 for $n=10$ and in Fig. 5 for $n=15$. By comparing with Fig. 1, it can be easily seen that the region stable to peeling-ballooning modes gets narrower as *n* increases, particularly in the

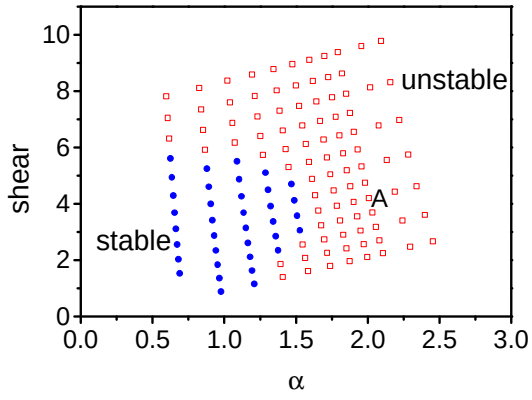

Figure 4. MHD stability of a JET diagnostic optimized configuration shot 55937 just before the type I ELM crash for n=10. Squares are unstable points and circles are stable ones. The point A corresponds to a reconstruction of the experimental equilibrium.

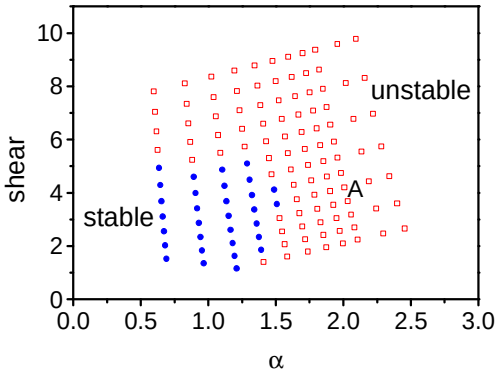

Figure 5. MHD stability of a JET diagnostic optimized configuration shot 55937 just before the type I ELM crash for n=15. Squares are unstable points and circles are stable ones. The point A corresponds to a reconstruction of the experimental equilibrium.

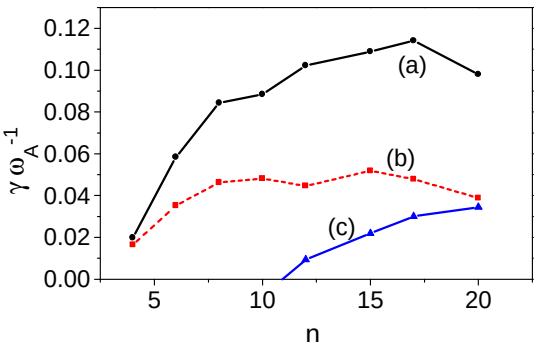

Figure 6. Growth rates of MHD modes normalized to Alfven time scale $\tau_A=R(\mu_0\rho)^{1/2}/B$ as a function of toroidal mode number n for
(a) equilibrium point A of Fig. 1,
(b) equilibrium point F of Fig. 1
(c) equilibrium point G of Fig. 1

low α *(α<1.5)*, high *s (s>5)* region and in the mid α *(1.3<α<1.8)*, mid *s (2<s<5)* region. Stability of the low *s* region is less sensitive to a change of *n*. The dependence of growth rate, γ, as a function of *n* for equilibrium points A, F, and G of Fig. 1 is shown in Fig. 6. For the experimental equilibrium A of shot 55937 (Fig. 6a), γ reaches a maximum at *n=17*. For the low shear case (Fig. 6b), γ has its maximum at lower *n* (*n=15*), while γ increases with *n* in the range studied for the large shear case (Fig. 6c).

Summary and Discussions

We have revisited the plasma edge stability analysis of a discharge in the JET diagnostic optimised configuration. The analysis shows that our results with the ELITE code are in good agreement with previous ones from the MISHKA code, both qualitatively and quantitatively. This enables the computing time to be significantly reduced and the real time analysis of edge MHD stability can be made possible for controlling ELMs actively in future tokamak experiments. ELITE also allows the analysis to be extended to high toroidal mode numbers without computations becoming too demanding on computing requirements. The stable region in *s*-α space gets narrower for higher *n* values. High *n* calculations need large memory and rather long computational time. However, it is necessary to analyze other experimental cases to make a large enough database to understand the ELM triggering mechanism.

Acknowledgement: This work was funded jointly by Daegu University (South Korea), the United Kingdom Engineering and Physical Sciences Research Council and the European Communities under the contract of Association between EURATOM and UKAEA. The views and opinions expressed herein do not necessarily reflect those of the European Commission. This work was carried out within the framework of the European Fusion Development Agreement.

References

[1] S. Saarelma et al., Plasma Phys. and Contr. Fusion **47** (2005) 713.
[2] A.B. Mihailovskii et al., Plasma Phys. Rep. **23** (1997) 844.
[3] A. Kallenbach et al., Plasma Phys. and Contr. Fusion **46** (2004) 431
[4] H.R. Wilson , P.B. Snyder, G.T.A. Huysmans and R.L. Miller Phys. Plas. **9** (2002) 1277.